LCMS for Analysis of Phosphorylation Sites of RIPK3 Inhibited by UH15-38

A thesis submitted by

Yulia Dikusar

in partial fulfillment of the requirement for the degree of

Master of Science

in

Pharmacology and Drug Development

Tufts University

Graduate School of Biomedical Sciences

August 2024

Advisor: Alexei Degterev, Ph.D.

Abstract

Necroptotic inflammation is an undesirable event in a wide range of disease areas including viral infections, neurodegenerative disorders and inflammatory bowel diseases. Receptor interacting protein kinase 3 (RIPK3) promotes necroptosis in a kinase dependent manner, through autophosphorylation and subsequent phosphorylation of mixed lineage kinase like (MLKL) protein. As the kinase activity of RIPK3 is independent of its apoptosis-promoting function, a RIPK3 kinase inhibitor could be a promising therapeutic agent. UH15-38 is a selective and potent RIPK3 inhibitor that prevents necroptosis and the consecutive damage in alveolar epithelial cells in vivo that was caused by severe Influenza A (IC50 = 39.5 nM). The mechanism of action of UH15-38 is not yet fully understood, but one of the hypotheses is that it inhibits an autophosphorylation site of RIPK3, halting its downstream activity. Thus, we employ liquid chromatography - mass spectroscopy (LCMS) phosphopeptide mapping to investigate the role of UH15-38 in inhibiting autophosphorylation sites of RIPK3. While mass spectroscopy provides a highly sensitive and rapid method to detect and evaluate phosphorylation sites (p-sites), it has limitations that require the analyte of high purity, concentration and reproducibility. To address this, we: examined the infection strategies of Sf9 suspension cells to produce a recombinant human RIPK3 of sufficient concentration and of correct folding such as decreasing the amount of p4 baculovirus used for expression and incubating infected Sf9 cells with the RIPK3 inhibitor; optimized digestion protocol, LCMS method and peptide mapping parameters to enhance the coverage and the number of matched hits. While the results do not give a definitive indication of the p-site of interest and require further troubleshooting, here we show possible optimization strategies as well as avenues for future focused studies.

Acknowledgements

Advisor: Alexei Degterev

Thesis Reader: David J. Greenblatt

Chris Singleton, Rachel Covitz, Ioannis Siokas and Peiyun Sang for their kindness and support.

Table of Contents

List of Tables

List of Figures

List of Abbreviations

ACN	Acetonitrile
Ambic	Ammonium Bicarbonate
CID	Collison-induced dissociation
cIAP1/2	cellular Inhibitor of Apoptosis proteins 1/2
DAMPs	Damage-associated molecular patterns
DMSO	Dimethyl sulfoxide
DTT	Dithiothreitol
EAD	Electron activated association
FADD	Fas-associated death domain protein
FASP	Filter Aided Sample Preparation
Guani	Guanidination
IAA	Iodoacetamide
IAV	Influenza A virus
INFɣ	Interferon-gamma
LC-MS/MS	Liquid chromatography – tandem mass spectrometry
LUBAC	Linear ubiquitin chain assembly complex
Lys-C	A sequencing grade enzyme hydrolyzing at carboxyl side of lysines
MEFs	Mouse Embryonic Fibroblast Cells
MLKL	Mixed lineage kinase domain like pseudokinase
m/z	mass-to-charge-ratio
MVM	Mass values matched
MVS	Mass values searched
NF-kB	Nuclear factor kappa-light-chain-enhancer of acticated B cells
p-site	Phosphorylation site
PTM	Post-translational modification
qToF	quadruple Time-of-Flight
RHIM	RIP homotypic interaction motif
RIPK1	Receptor-interacting protein kinase 1

RIPK3	Receptor-interacting protein kinase 3
SDS	Sodium dodecyl-sulfate
Sf9	Insect cell line
TCEP	Tris(2-carboxyethyl) phosphine
TFA	Trifluoroacetic acid
TNFα/TNFR	Tumor Necrosis Factor α/Tumor Necrosis Factor Receptor
TRAF2	TNF receptor-associated factor
ZBP1	Z-DNA-binding protein 1

Chapter 1: Introduction

1.1 Necroptosis and RIPK3

Cell death – a biological event in which the cell ceases to exist – could occur due to various stimuli. Scientists differentiate regulated cell death from accidental cell death, with the former having dedicated biological pathways that could be targeted pharmacologically.[1] Apoptosis and necroptosis are forms of regulated cell death. Apoptosis is the cell death that occurs through cell shrinkage and fragmentation with limited debris and content leakage. Necroptosis on the other hand is a programmed necrotic cell death that is highly pro-inflammatory due to plasma membrane rapture and consecutive release of damage-associated molecular patterns (DAMPs). Apoptosis supports normal development of organisms and mediates disease-associated cell death and inflammation to promote survival, whereas necroptosis is an aggressive defense mechanism against pathogens that causes a cascading damage to a point of lethality.[2]

Complex machinery is involved in the activation of necroptosis and apoptosis. Several signaling pathways could be stimulated to induce necroptosis, such as TNFa/TNFR, Fas ligand/FAS, interferon-gamma (INF-y), double stranded RNA/Toll like receptor 3 and double stranded DNA/Z-DNA binding protein 1 (ZBP1). The possible events downstream could be apoptosis, necroptosis and cell survival, with receptor-interacting protein kinase 1 (RIPK1) as important checkpoint protein. Ubiquitinated RIPK1 engages in a Complex I with TNFR1-associated death domain (TRADD), TNFR-associated factor 2 (TRAF2), cellular inhibitor of apoptosis proteins 1/2 (cIAP1/2) and linear ubiquitin chain assembly complex (LUBAC). If RIPK1 is ubiquitinated, cells will

survive through NF-kB activation by Complex I; if it is de-ubiquitinated, RIPK1 assembles Complex IIa with Fas-associated death domain protein (FADD) and caspase-8 in kinase-independent manner, and cells undergo apoptosis. In the absence of a functional caspase-8, RIPK1 phosphorylates and recruits to oligomerized RIPK3 which is facilitated by RIP homotypic interaction motif (RHIM) domain interactions. RIPK3 in turn undergoes autophosphorylation. Noteworthy, dimerization of RIPK3 could directly lead to its autophosphorylation.[3] The complex of RIPK1, RIPK3 and mixed lineage kinase domain like pseudokinase (MLKL), also known as necrosome, drives the phosphorylation of MLKL by RIPK3 and eventual dislocation of MLKL to the cell membrane. Further polymerization and oligomerization of MLKL enables its lipid-binding capacity and results in the disruption of the cell membrane and necroptotic cell death.[4]

1.2. UH15-38 as Inhibitor of RIPK3

The attempts to prevent necroptosis by inhibiting RIPK1 kinase function were not proven successful. For example, such inhibition accelerated atherosclerotic plaque formation in RIPK1 kinase-inactive ApoE-/- mice, and the pharmacological inhibition of RIPK1 kinase with GSK'547 in the ApoE-/- model of advanced atherosclerosis not only did not change the plaque size compared to control but additionally induced apoptosis.[5] Downstream of RIPK1, RIPK3 seemed a better pharmacological target as its kinase activity is assumed to be the only driver for necroptosis with MLKL as its final effector. Independent of its kinase function, RIPK3 is also associated with activation of inflammasomes and apoptosis.[6] Inhibiting the kinase domain of RIPK3 might prove beneficial in preventing necroptosis while still permitting apoptosis to occur.

Gautam, Boyd et al introduced UH15-38, a new RIPK3 kinase inhibitor that outperforms (IC50 = 98 nM) the previous best-performing GlaxoSmithKline inhibitor (GSK'872, IC50 = 582 nM) and is potent both in vitro against recombinant RIPK3 and in vivo in human and mouse cell lines.[7] This enhanced efficacy in inhibiting tumor necrosis factor (TNF)-induced necroptosis was initially discovered through screening analogues of PD166285 in mouse embryonic fibroblasts (MEFs).[7] UH15-38 shows specificity for RIPK3-driven necroptosis and maintains an S(35) selectivity score (approximately 0.25) comparable to clinically approved tyrosine kinase inhibitors across a panel of 90 human kinases.[7] Additionally, it demonstrates no significant inhibition of 50 proteins typically associated with severe side effects.[7] In vivo tests on wild-type mice demonstrated good efficacy, with intraperitoneal injections of UH15-38 at doses of 30 mg/kg for seven days, with the compound predominantly accumulating to significant levels in the lung, liver, heart, kidney and colon tissues. In $Casp8^{-/-}Mlkl^{Flag/Flag}$ mice, a model that enables the detection of phosphorylated MLKL without animals succumbing to necroptosis, UH15-38 effectively blocked MLKL phosphorylation.[7] Dosed intraperitoneally for seven consecutive days at 30 mg kg^{-1} day^{-1}, compound was exceptionally well tolerated in vivo with no marked signs of on-target apoptosis or general toxicity.[7] With only the exception of neurological disorders due to limited blood-brain barrier permeability, this data suggests that the UH15-38 could be therapeutically applied to a wide range of disorders.

1.3. Possible Therapeutic applications of UH15-38

Necroptosis contributes to a plethora of disease pathologies, such as neurodegenerative, cardiovascular, malignant, inflammatory and infectious diseases.[8] For example, conditions like Inflammatory Bowel Disease (IBD) could benefit from RIPK3

inhibitors, as necroptosis has been implicated in the pathogenesis of these diseases. By inhibiting RIPK3, the inflammatory cascade that leads to tissue damage and the symptoms of IBD might be mitigated.[9]

RIPK3 was shown to activate both necroptotic and apoptotic death in parallel manner following the infection of fibroblasts and lung epithelial cells with Influenza A virus (IAV), which is the most prominent driver of influenza in birds and mammals.[10] Inhibition of the RIPK3 kinase activity with UH15-38 was assessed in MLKL-deficient mice, that was infected with a lethal dose of IAV and monitored over a course of three-weeks, and it was found that 70% of necroptosis-deficient mice made a full recovery.[7]

1.4. Phosphorylation of RIPK3 and the Challenges of Detection

The mechanism of action of UH15-38 has not yet been elucidated. Gautam, Boyd et al proposed that the ability of the phenol of UH15-38 to interact with the back pocket of RIPK3 and thus inhibit the displacement of the αC helix, that is required for binding with MLKL, is what drives its potency both *in vivo* and *vitro* .[7] Here, we speculate that UH15-38 blocks a certain RIPK3 autophosphorylation site, resulting in inhibition of necroptosis.

It is well established that phosphorylation is a vital post-translational modification that drives various cellular processes. However, its detection presents significant challenges due to the typically low abundance of phosphorylated proteins and the transient nature of phosphorylation events. Efficient detection requires samples with sufficient concentration and quality, as minor modifications like the loss of 80/98 Da (corresponding to the mass of a phosphate group) can indicate phosphorylation.[11]

Liquid chromatography-mass spectrometry (LC-MS) is a highly sensitive technique for detecting phosphorylation. Advancements like the Orbitrap and time-of-

flight (ToF) mass spectrometers have set new standards in sensitivity and accuracy. The ToF allows for the precise measurement of mass-to-charge ratios with high resolution and accuracy, facilitating the detection of subtle changes like phosphorylation.[12] However, despite these technological advances, challenges remain. These include issues with ion suppression, incomplete coverage, and the limitations of dynamic range of detection, which can obscure low-abundance species in complex biological samples.[13]

To mitigate some of these complications, the analysis of a single isolated protein might be particularly beneficial. Focusing on the individual, recombinantly expressed protein allows for a controlled analysis environment where the concentration of phosphorylated species is enhanced relative to the background, potentially reducing issues related to sensitivity and specificity. The LC-MS method itself requires careful optimization to ensure effective separation and accurate detection of phosphorylated peptides. The choice of enzyme for protein cleavage, such as trypsin, is vital, as it must efficiently cleave proteins while preserving phosphorylation sites. Additionally, the selection of chromatographic columns is crucial; columns that minimize nonspecific binding can significantly improve the detection of phosphorylated peptides.[14] This comprehensive approach should improve the detection of phosphorylation and hopefully shed some light on the mechanism of action of UH15-38.

Chapter 2: Materials and Methods

2.1. Preparation of Recombinant RIPK3

To prepare the recombinant human RIPK3 kinase domain (residues 1-316) we expressed and purified it from Sf9 insect cells that we seeded at 3 million cells per mL, using C3S C110A p4 baculovirus as per established procedure.[15] We produced a hRIPK3 that contained N-terminally fused TEV protease-cleavable His6 tag, which facilitated the Ni-assisted purification and dialysis of lysed Sf9 cells. We quantified the purified protein by NanoDrop and analyzed by Western blot.

2.2. Antibodies

We used the following primary antibodies: anti-human-phospho-S227-RIPK3 rabbit monoclonal (Abcam, ab209384); anti-human-phospho-S358-MLKL rabbit monoclonal EPR9514 (Abcam, ab187091); anti-human-RIPK3 mouse monoclonal (RnD Systems, MAB7604), anti-human-MLKL rabbit monoclonal EPR17514 (Abcam, 184718) and anti-6xHis-Tag mouse monoclonal (Invitrogen, MA1-21315). We used two secondary antibodies: anti-rabbit IgG (H + L) DyLightTM 800 4X PEG Conjugate (Cell Signaling, 5151), anti-mouse IgG (H + L) DyLightTM 800 4X PEG Conjugate (Cell Signaling, 5257). Antibody dilutions were 1:1000 for primary and 1:30000 for secondary antibodies.

2.3. Reagents

For Sf9 cells media: Sf-900™ II SFM, Sf-900™ III SFM (Gibco). Enzymes: Trypsin, Trypsin/Lys-C. De-phosphorylation: Lambda Protein Phosphatase (New England BioLabs, S P0753S). Immunoprecipitation: Dynabeads His-Tag Isolation & Pulldown (Invitrogen, 10103D). Solvents: 0.1% Formic acid in Acetonitrile LC-MS grade, 0.1%

Formic acid in Water, LC-MS grade (Thermo Scientific, LS120500 and LS118500). TFA Optima LC-MS Grade (Fisher Chemical, AAB-A116). Kinase reactions: Ultra Pure ATP 10 mM (Promega, V915B-C); UH15-38 was scaled-up at University of Texas at San Antonio Center of Innovative Drug Discovery.

2.4. Kinase reactions

We run kinase reactions in the following manner: to recombinant hRIPK3 (1-316 a.a) added 5x kinase buffer (final 1x kinase buffer is 200 mM Tris pH 7.5, 100 mM $MgCl_2$), LCMS-grade water, 10 μM UH15-38 or DMSO diluted in water, waited 5-7 min and added 50 μM ATP or water; incubated for 30 min at RT. Taken down for LCMS digestion. To all (if not conducted LCMS analysis on the samples) or to a portion added 4X SDS, boiled for 5 min at 95 C and stored at -20 C until ready to use. We run the 15% gels and probed with corresponding human antibodies.

2.5. Digestion

We explored several digestion methods: in-gel digestion (UWPR Proteomics Resource "In-gel digestion") and In-Solution Digestion (UWPR Proteomics Resource "Protein Reduction, Alkylation, Digestion"). The following kits were employed: "In-solution Tryptic Digestion and Guanidination Kit (Thermo Scientific, 1859663); "FASP Protein Digestion Kit" (Abcam, ab270519), "Pierce C18 Spin Columns (Thermo Scientific, 89870). We digested the recombinant protein samples, provided in 25 mM TrisHCl, pH8, 150 mM NaCl, 1 mM MgCl2, 10% glycerol and 0.1 mM PMSF buffer after purification, using one of the digestion methods below. For all digests we used ultrapure water and LC-MS grade solvents.

2.5.1. In-gel digestion (Based on UWPR Proteomics Resource “In-gel digestion”):

1. Post kinase reaction for the samples in 1X SDS, we run Coomassie SDS-PAGE (overnight stain) to visibly mark the bands of interest.
2. Decontaminated the work area and tools with 70% Acetonitrile in ultrapure water and then 1% Acetic acid in ultrapure water.

   Took the following steps for each sample (used equal amounts of solutions for all samples).
3. Cut out the band of interest with razor blade, added to the 1.5 mL Eppendorf tube, washed with 50% acetonitrile & 50 mM Ambic (Ammonium Bicarbonate) in ultrapure water: submerged the gel piece, incubated for 15 min at 37° C, discarded and repeated 1 time to wash the dye away.
4. Resubmerged the gel piece in 100% Acetonitrile, which after 5 minutes turned opaque.
5. Removed the Acetonitrile and leaved on the heating rack for 5 min at 37°C to remove the remainer of the solvent.
6. Added 10 mM DTT in 100 mM Ambic, incubated for 30 min at 56° C, with Eppendorf tubes sealed with parafilm.
7. Repeated steps 4-5. Washing and drying of the gels completed once the gels turned opaque.
8. Added 55 mM IAA, incubated for 20 min in the dark at room temperature.
9. Washed with 100 mM Ambic once, and repeated steps 4-5.
10. Resubmerged the gel piece in 5 µg/mL Trypsin in 50 mM Ambic, incubated overnight at 30C, with tubes sealed with parafilm.

11. The next day, cooled the sample for 5 min at -4° C, with parafilm on.
12. Sonicated in a bath for 10 min on a floating rack with parafilm still on to diffuse the peptides of the gel.
13. Decontaminated the tubes, still in parafilm with 70% Acetonitrile in ultrapure water and then 1% Acetic acid in ultrapure water.
14. Removed the parafilm and transferred the supernatant from each tube to new set of tubes. Kept at -80° C until further treatment.
15. Performed C18 clean up using the C18 Zip tips, with elution in 0.1% TFA & 70% Acetonitrile in ultrapure water to LCMS vials.
16. Removed the solvent on Genevac and resuspended in 2% acetonitrile (ACN) with 1% formic acid (FA) in ultrapure water. Kept frozen until analysis.

2.5.2. In-Solution Digestion (UWPR Proteomics Resource "Protein Reduction, Alkylation, Digestion"):

1. Post kinase reaction for each sample, added Ambic and Urea to a final concentration of 6 M Urea in 100 mM Ambic.
2. Added DTT to a final concentration of 5 mM in solution and incubated for 45 min at 56°C (not higher than 60°), sealed in parafilm.
3. Cooled down at room temperature and spun down briefly.
4. Added IAA to 14 mM final concentration, incubated for 30 min at room temperature in the dark.
5. Added DTT to the concentration of additional 5 mM in solution, incubated for 15 min at room temperature in the dark.
6. Diluted the sample 1:5 in 100 mM Ambic to reduce Urea concentration.

7. Added calcium chloride to a 1 mM concentration in solution.
8. Added Trypsin solution to obtain 2 µg of Trypsin in each vial, incubated overnight at 37°C.
9. Added 0.4% (v/v) TFA, verified that pH was lower than 2 with pH paper.
10. Centrifuged at 2500 x g for 10 min at room temperature, transferred the supernatant to LCMS vials, discarded the pellet. Kept frozen until further processing.
11. Dried in Genevac and resuspended in 2% acetonitrile (ACN) with 1% formic acid (FA) in ultrapure water. Kept frozen until analysis.

2.5.3. "In-solution Tryptic Digestion and Guanidination Kit (Thermo Scientific, 1859663):

Note: the kit recommended using 10.5 uL of sample, we used double of that for each sample, also doubling all amounts recommended in the kit instructions. Used only the materials from the kit. We stored 100 µg Trypsin/Lys-C in 100 µL 0.1% Acetic acid in H_2O, aliquoted to 10 µL in individual vials.

1. Denatured/alkylated at 95°C for 10 min using 20 mM DTT in ~30 mM Ambic.
2. Alkylated in the dark at room temperature for 20 min using 40 mM IAA.
3. Digested at 37°C overnight using 1 µg of Trypsin or Trypsin/Lys-C per sample.
4. Guanidinated the entire digest or half (added ultrapure water to both samples to bring up to the same final volume before LCMS analysis; did not add guanidination reagents to control) at 65C for 12 minutes following the procedure detailed in Instructions for "In-Solution Tryptic Digestion and Guanidination Kit.

5. Stored at -20C until LCMS analysis.

2.5.4. “FASP Protein Digestion Kit” (Abcam, ab270519) in tandem with “In-solution Tryptic Digestion and Guanidination Kit (Thermo Scientific, 1859663):

Note: in this method we used 30 kDa MWCO spin filters to perform the digestion on. We used materials provided by both kits, which protocols we merged.

1. We performed kinase reactions (22 µL total volume each reaction), took 20 uL and added Urea and TCEP in Tris-HCl pH 7 to a final concentration of 6 M Urea and 10 mM TCEP in 100 mM Tris-HCl pH 7 and 30 µL total volume.
2. Denatured/alkylated for 10 min at 95°C, allowed the sample to cool.
3. Mixed up all of each sample with 200 µL of ~15 M Urea in 100 mM Tris-HCl solution and centrifuged at 14,000 x g for 15 minutes.
4. Added another 200 µL of ~15 M Urea in 100 mM Tris-HCl solution to the Spin Filter and centrifuged at 14,000 x g for 15 minutes.
5. Discarded the flow-through from the collection tube.
6. Added ~53 mM Iodoacetamide Solution in ~15 M Urea in 100 mM Tris-HCl solution to the Spin Filter and vortexed for 1 minute; incubated without mixing for 20 minute in the dark.
7. Centrifuged the Spin Filter at 14,000 x g for 10 minutes.
8. Added 100 µL of ~15 M Urea in 100 mM Tris-HCl solution to the Spin Filter and centrifuged at 14,000 x g for 15 minutes.
9. Repeated this step twice. Discarded the flow-through from the collection tube.

10. Added 100 µL of 50 mM Ammonium Bicarbonate Solution provided in the kit to the Spin Filter and centrifuged at 14,000 x g for 10 minutes. Repeated this step twice.
11. Added 75 µL of digestion solution (5 µL of 1 µg/µL Trypsin/Lys-C plus 295 uL 50 mM Ambic) to each Spin Filter and vortexed for 1 minute. Wraped the tops of the tubes with parafilm to minimize the effects from evaporation.
12. Incubated the Spin Filter on a heated rack at 37°C for 12-18 hours.
13. Transferred the Spin Filter to a new collection tube.
14. Added 40 µL of 50 mM Ammonium Bicarbonate Solution.
15. Centrifuged the Spin Filter at 14,000 x g for 10 minutes. Repeated this step once.
16. Added 50 µL of 0.5 M Sodium Chloride Solution provided and centrifuged the Spin Filter at 14,000 x g for 10 minutes.
17. Acidified the filtrate that contained the digested proteins with TFA to pH ~2-3.
18. Centrifuged at 2,500 x g for 10 min at room temperature and discarded the pellet.
19. Concentrated the supernatant on Genevac, resuspended in 50% Acetonitrile & 0.1% TFA in ultrapure water and performed Guanidination as mentioned above, using “In-Solution Tryptic Digestion and Guanidination Kit.
20. Dried the samples on Genevac and resuspended in 2% acetonitrile (ACN) with 1% formic acid (FA) in ultrapure water. Kept frozen until analysis.

2.5.5. “FASP Protein Digestion Kit” (Abcam, ab270519) in tandem with Pierce C18 Spin Columns (Thermo Scientific, 89870):

Note: in this method we used 30 kDa MWCO spin filters to perform the digestion on. We used materials provided by both kits, which protocols we merged.

21. We performed kinase reactions (22 µL total volume each reaction), took 20 uL and added Urea and TCEP in Tris-HCl pH 7 to a final concentration of 6 M Urea and 10 mM TCEP in 100 mM Tris-HCl pH 7 and 30 µL total volume.
22. Denatured/alkylated for 10 min at 95°C, allowed the sample to cool.
23. Mixed up all of each sample with 200 µL of ~15 M Urea in 100 mM Tris-HCl solution and centrifuged at 14,000 x g for 15 minutes.
24. Added another 200 µL of ~15 M Urea in 100 mM Tris-HCl solution to the Spin Filter and centrifuged at 14,000 x g for 15 minutes.
25. Discarded the flow-through from the collection tube.
26. Added ~53 mM Iodoacetamide Solution in ~15 M Urea in 100 mM Tris-HCl solution to the Spin Filter and vortexed for 1 minute; incubated without mixing for 20 minuts in the dark.
27. Centrifuged the Spin Filter at 14,000 x g for 10 minutes.
28. Added 100 µL of ~15 M Urea in 100 mM Tris-HCl solution to the Spin Filter and centrifuged at 14,000 x g for 15 minutes.
29. Repeated this step twice. Discarded the flow-through from the collection tube.
30. Added 100 µL of 50 mM Ammonium Bicarbonate Solution provided in the kit to the Spin Filter and centrifuged at 14,000 x g for 10 minutes. Repeated this step twice.

31. Added 75 µL of digestion solution (5 µL of 1 µg/µL Trypsin/Lys-C plus 295 uL 50 mM Ambic) to each Spin Filter and vortexed for 1 minute. Wraped the tops of the tubes with parafilm to minimize the effects from evaporation.
32. Incubated the Spin Filter on a heated rack at 37°C for 12-18 hours.
33. Transferred the Spin Filter to a new collection tube.
34. Added 40 µL of 50 mM Ammonium Bicarbonate Solution.
35. Centrifuged the Spin Filter at 14,000 x g for 10 minutes. Repeated this step once.
36. Added 50 µL of 0.5 M Sodium Chloride Solution provided and centrifuged the Spin Filter at 14,000 x g for 10 minutes.
37. Acidified the filtrate that contained the digested proteins with TFA to pH ~2-3.
38. Wetted (with 50% acetonitrile in water) and equilibrated (with 5% CAN & 0.5% TFA in water) the resin of C18 Spin Columns according to the procedure. Repeated each step 1 time.
39. Loaded the samples on resin in columns that were labeled accordingly, centrifuged at 1,500 x g for 1 minute and repeated 1 time.
40. Washed the resin with 0.5% TFA & 5% acetonitrile in water solution, centrifuged at 1,500 x g for 1 min, discarded flow-through and repeated 2 times.
41. Placed the columns in new receiver tubes, eluted with 20 µL 70% acetonitrile twice (total 40 µL).
42. Transferred to LCMS vials, concentrated on Genevac, resuspended in 2% acetonitrile (ACN) with 1% formic acid (FA) in ultrapure water. Kept frozen until analysis

2.6. Western Blot

For Western Blotting we denatured the samples by adding SDS sample buffer and boiling for 5 min, and loading ~0.5 µg of protein into each well on the gel. We transferred the proteins to polyvinylidene diflouride membranes (Millipore, Immobilon transfer membrane, Bedford, MA, USA). After blocking with 5% milk in 0.1% Trisbuffered saline Tween (TBS-T) (10 mM Tris-HCl pH 7.6, 150 mM NaCl, 0.1% Tween 20) for 1 h, incubated the membranes overnight at 4 °C with primary antibodies, washed, incubated with secondary antibodies, washed again and scanned on LI-COR western blot scanner.

2.7. Mass Spectrometry

We kept the digested samples, resuspended in 2% acetonitrile (ACN) with 1% formic acid (FA), frozen until analysis on ZenoToF 7600 LC-MS/MS and ExionLC system (Sciex, USA) with EAD or CID fragmentation modes. We separated the peptides on 2.1x100 mm analytical ACQUITY UPLC CSH, with 1.7 µm C18 beads 50 °C, 0.3 mL/min using a gradient from buffer A (99.9% Water, 0.1% FA) to buffer B (99.9% ACN, 0.1% FA; 74 min). We included the complete LCMS instrument method in the Appendix.

2.8. Processing method

We processed the wiff2 files from the LC-MS/MS analysis on Biologics Explorer 3.0 (Sciex, USA) with provided sequence of recombinant RIPK3 as a reference. Tested with Trypsin and Trypsin/Lys-C enzymes, with fixed carbomidemethyl modification (C) and guanidinyl modification (K) in case of guanidination treatment. We included the complete LCMS method in the appendix.

2.9. Immunoprecipitation

For Concentration of Original Stock: we concentrated the 170 µL of 0.5 mg/mL recombinant hRIPK3 (1-316 a.a) to 2.83 mg/mL (30 µL) using Amicon Ultra - 0.5 mL 3K Ultracel-3K membrane for 2.25 hrs at 4C and 14,000 x g. To 1 µL from concentrated RIPK3 stock we added 20 µL H_2O, 7 µL 4 x SDS, boiled for 5 min at 95 C and stored at -20 C until Western blot. To 7.3 µL of hRIPK3 in 1x kinase buffer (200 mM Tris pH 7.5, 100 mM $MgCl_2$) we added 55 µM UH15-38 or DMSO in H_2O, waited 5 min and added 50 µM ATP or H_2O for total volume of 11.5 µL; 30 min at RT. To 1 µL from each sample added 17 µL 1X SDS, boiled for 5 min at 95 C and stored at -20C until Western blot. The rest of the samples we stored at -20C until digestion. Run 15% gel with ~0.5 µg of protein per well, and probed with human ph-RIPK3.

For De-phosphorylation of Autophosphorylated Stock:

1. Elution buffer: 300 mM Imidazole, 20 mM Tris pH 8.0, 300 mM NaCl, 0.01% Tween™-20. Wash buffer: 20 mM Tris pH 8.0, 300 mM NaCl, 0.01% Tween™-20. Beads: Dynabeads™ His-Tag 10103D.
2. Stock: to 1 µL of 2.8 mg/mL recombinant hRIPK3 (1-316 a.a) added 20 µL H_2O and 7 µL 4x SDS, boiled at 95C for 5 min and stored at -20C until Western.
3. On Beads: aliquoted 60 µL of beads, washed 3x times, incubated 27 µL of with 120 µL wash buffer, incubated at RT for 10 min, washed 2x with wash buffer, resuspended in 150 µL wash buffer and collected 5.6 µL bead slurry with 15.4 µL H_2O and 7 µL 4x SDS, boiled at 95C for 5 min and stored at -20C until Western.

4. Lambda Phosphatase: washed the remainder beads 2x with 1x NEBuffer for Protein MetalloPhosphotases (PMP) with 1 mM $MnCl_2$, incubated for 1 hr in 50 µL (3 µL of Lambda phosphatase per sample) at 30C and 800 rpm, washed 2x with wash buffer, resuspended in 50 µL, collected 1 µL bead slurry with 20 µL H_2O and 7 µL 4x SDS, boiled at 95C for 5 min and stored at -20C until Western.
5. Kinase Buffer: resuspended the remainder beads in 25 µL 1x kinase buffer (200 mM Tris pH 7.5, 100 mM $MgCl_2$), aliquoted 1 µL with 17 µL 1x SDS, boiled at 95C for 5 min and stored at -20C until Western.
6. Kinase Reactions: aliquoted 7.3 µL of resuspended bead slurry in 1x kinase buffer, added 55 µM UH15-38 or DMSO in H_2O, waited 5 min and added 50 µM ATP or H_2O for total volume of 11.5 µL; 30 min at RT. Removed the buffer and resuspended in 11.5 µL elution buffer, waited 5-7 min at RT and removed beads. Aliquoted 1 µL with 17 µL 1x SDS, boiled at 95C for 5 min and stored at -20C until Western.

2.10. Collaboration

We thank Peiyun Sang for performing the lysis of Sf9 cells and the consequent isolation, purification and concentration of the recombinant protein. All experiments, digestions and analysis was performed by Yulia Dikusar.

Chapter 3: Results

3.1. Initial Assessments of RIPK3 phosphorylation sites

To assess the mechanism of action of RIPK3 we employed the kinase assays with three different conditions. The conditions and expectations for each sample are listed in Table 3.1 below. Fetuin was used as initial validation that LCMS equipment at our disposal was usable to detect and analyze digested samples and match them with existing amino acid sequence.

Table 3.1. Conditions and expectations for RIPK3 kinase reactions.

Protein	**Condition**	**Expectations**
Fetuin	Control	Digested Control Sample
Recomb. hRIPK3	With ATP	Should observe RIPK3 autophosphorylation
	No ATP	No RIPK3 autophosphorylation (no ATP was added so no kinase reaction took place)
	With ATP & UH15-38	No RIPK3 autophosphorylation (this was a kinase reaction with ATP, but in the presence of RIPK3 inhibitor - UH15-38)

Initially synthesized recombinant human RIPK3 (0.5 mg/mL, Stock A) was used to perform kinase reaction with 1 μM UH15-38 and low (20 ng) and high (100 ng) amounts of protein (Fig 3.1.B). Two distinctive bands corresponding to phosphorylated RIPK3 are visible upon addition of ATP, and only one band remains under condition where UH15-38 is added before ATP. At the same time, phosphorylation of MLKL is reduced in the samples treated with UH15-38 suggesting a corresponding inhibition of necroptosis. This finding prompted us to examine whether UH15-38 functions through inhibition of a certain p-stie.

So far it has been reported that human RIPK3 T224 and especially S227 are autophosphorylation sites that strengthen interaction with MLKL which occurs as an independent event from MLKL phosphorylation, while phosphorylation at S176 is a result

of necroptotic signaling.[16] Overall, the three clusters of p-sites, located in the C-lobe of the kinase domain, were addressed by Meng et al: pT224/pS227, pS164/pT165 and pT182 but only the first two were shown to have significance.[16] The recombinant human RIPK3, that is used in our analysis, contains residues up to 316 amino acids, so these regions could be examined as well.

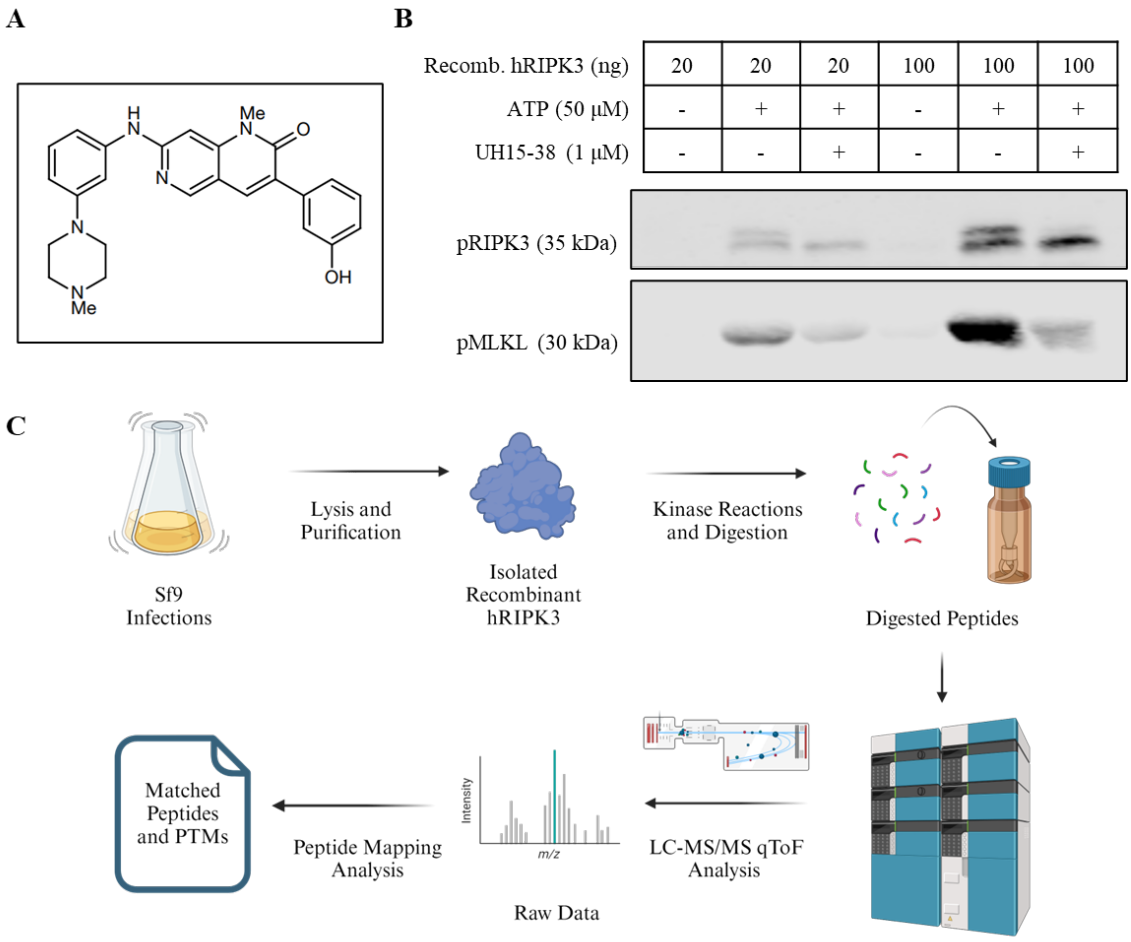

Fig. 3.1. Analysis of UH15-38 as inhibitor of RIPK3 autophosphorylation.
A. Structure of UH15-38. B. Kinase assay with 20 and 100 ng of human RIPK3 that display effect of UH15-38 on autophosphorylation of RIPK3. C. Workflow layout for detection of phosphorylated sites of RIPK3; created with BioRender.

The workflow for the analysis of the phospho-sites is shown on Fig. 3.1.C. The first digestion protocol we explored was in-gel digestion post SDS-PAGE, with the sections of

interest visualized with Coomassie Blue stain with C18 Zip tip clean up. This prep did not yield any measurable results as no protein signal showed up on LCMS. So, we explored in-solution digestion, speculating that the amount of protein on the gel was too low, and chose against C18 treatment to avoid any additional loss of protein. We followed UWPR Proteomics Resource "Protein Reduction, Alkylation, Digestion" using in-house urea, iodoacetamide (IAA) and dithiothreitol (DTT). The original stock of hRIPK3 that we expressed and purified was of 0.5 mg/mL concentration, and this was the limiting factor for amount of protein we could digest at a time and thus inject on the LC-MS. The results for the original LC-MS analysis are shown in Fig. 3.2.A and B below.

A

Recomb. hRIPK3	ATP	UH15-38	Coverage (%)	CID/ EAD	MVS	MVM	Inj. Vol (uL)	RIPK3 per Inj. (ug)	Guani.	Treatment
Stock A 0.5 mg/mL	-	-	97.9	CID	3326	214	20	2	-	Trypsin
	+	-	93.8	CID	3326	214				
	+	+	98.5	CID	2881	147				
	-	-	98.5	CID	2916	155				
	+	-	95.9	CID	2479	124				
	+	+	98.5	CID	2776	146				
	-	-	71.8	EAD	1454	37	40	6	+	Kit with Trypsin
	+	-	75.9	EAD	1662	48				
	+	+	80.2	EAD	1233	33				
	-	-	76.5	EAD	1454	28	40			
	+	-	76.5	EAD	1662	33				
	+	+	79.1	EAD	1233	24				
	-	-	86.0	CID	1435	29	20	3		
	+	-	86.0	CID	1226	31		3		
	+	+	78.8	CID	959	21		3		

B

ATP	UH15-38	CID/EAD	Guani.	Treatment	S54	S66	S108	T224	S311
-	-	CID	-	Trypsin		1.41	21.57	18.77	
+	-	CID			11.58		22.87	27.93	
+	+	CID				0.87	16.79	14	3.18
-	-	EAD	+	Kit with Trypsin			15.15	18.08	
+	-	EAD					12.89	18.27	
+	+	EAD			100			17.04	
-	-	EAD						17.09	
+	-	EAD						21.26	
+	+	EAD							
-	-	CID			100				
+	-	CID						19.85	
+	+	CID							

Fig. 3.2. Results of human RIPK3 phopshopeptide mapping analysis.
A, B. The conditions tested along with the following parameters: coverage % of amino acid sequence, CID or EAD fragmentation pattern, mass values searched (MVS), mass values matched (MVM), injection volume, amount of RIPK3 per injection, guanidination treatment (Guani.); detected phosphorylation sites are adjusted to match the human sequence, values in green represent relative volume of each phosphorylated site.

Mass values searched (MVS), mass values matched (MVM) and percent coverage are the indicators of how well the software matched the provided amino acid sequence with the ionized peptides it detected. Ideally, we want to maximize the coverage, and possibly MVS and MVM, however, too many searched peptide fragments could be a sign of high background noise and is arguably not ideal.[17]

The results we received were challenging to interpret, as the repeats were not reproducible, did not have consistent MVS and MVM, while the detected phosphorylation events not only did not match our expectations for the site of interest that we stated in Table 3.1 but also showed phosphorylation modifications in cases where we expect none (Fig 3.2.A and B in blue). We attempted to utilize guanidination and equip a standardized kit from Thermo Scientific to improve consistency of the sample preparation and ionization of the tryptic peptides after guanidinyl modification.[18] We also focused on EAD fragmentation mode instead of CID to see if it would improve the detection of phosphorylation events. However, we observed an up to 15% decrease in coverage and 4-6 fold decrease in MVM values compared to the previous experiment. Additionally, CID fragmentation method did not show a significant advantage over EAD in terms coverage and had lower amount of phosphorylation events detected overall compared to EAD (Fig 3.2.A and B gray). While the site S136, which corresponds to S108 in human sequence of RIPK3, did seem to be less phosphorylated in the 2 instances of measurements, we were unable to draw definitive conclusions at the time. As a result, we looked into more methods to improve detection. One possible option was to prepare a recombinant RIPK3 of higher concentration to load more protein on the LCMS column at once and thus have a better

chance of detecting phosphorylation modifications, which are commonly low in abundance.[19]

3.2. Autophosphorylation of RIPK3 and UH15-38 as a chaperone in Sf9 culture

When using a higher amount of p4 baculovirus to achieve a higher recombinant protein expression in Sf9 cells, we observed a highly autophosphorylated RIPK3 which could be seen on Fig 3.3.A. It seemed that the amount of observed phosphorylation of RIPK3 was sufficient to drive phosphorylation of MLKL, even in the presence of UH15-38.

To mitigate this issue, we employed several strategies. First, we examined the possibility of concentrating the original stock of hRIPK3 from 0.5 mg/mL up to 5-fold using Amicon Ultra - 0.5 mL 3K Ultracel-3K membrane. This was done successfully as could be seen on Fig. 3.3.B; however, the amount of concentrated protein was fairly limited to run a series of digestions and to allow for replicates.

Second, we explored the option of His-tag driven immunoprecipitation to de-phosphorylate already produced recombinant protein using lambda phosphatase. While de-phosphorylation did occur, as could be seen from the sample of the Lamba phosphatase-treated protein in the NEB buffer on beads on Fig. 3.3.B, the protein sample post transfer to the kinase buffer and prior to the kinase reactions showed noticeable amount of phosphorylation. It could be argued that this sample contained more protein than the previous one with lambda phosphatase, and thus more phosphorylation was observed. Nevertheless, this protocol required a significant amount of lambda phosphatase which did not seem optimal. Additionally, imidazole elution buffer did not successfully release the

protein off the beads after kinase reactions. Exploring this avenue further, we tested several elution buffers with varying amounts of imidazole (Fig. 3.3.C); however, significant amount of protein still remained on the beads.

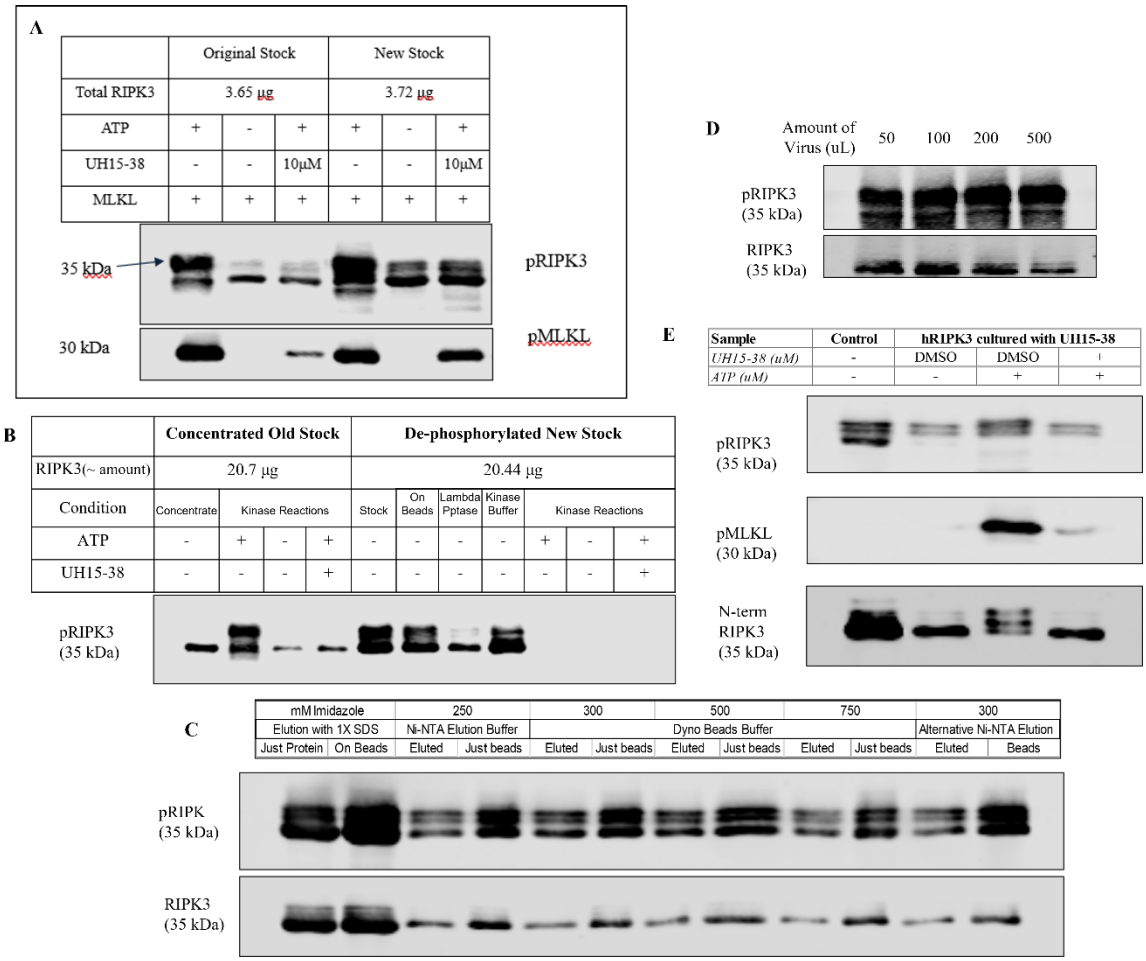

Fig. 3.3. Challenges with autophosphorylation of recombinant RIPK3. A. Comparison of old and new batches of recombinant human RIPK3. B. Strategies to produce de-phosphorylated stock of RIPK3 of high enough concentration; first 4 lanes correspond to the concentration experiment with Amicon membranes, last 7 lanes – to the IP experiment aimed to use lambda phosphatase to dephosphorylate RIPK3. C. Screening of available elution buffers with varying amounts of imidazole. D. Observed autophosphorylation of RIPK3 when 50-500 µL of virus is used. E. UH15-38 as a chaperone of RIPK3 during Sf9 infection, Control is the autophosphorylated RIPK3.

Third, we attempted to decrease the amount of the p4 baculovirus added to Sf9 suspension cells, hoping to achieve the perfect amount for sufficient expression of RIPK3

that is not significantly autophosphorylated. Example of the observed autophosphorylation of RIPK3, that occurred from infection with hRIPK3 1-316 aa C3S C110A P4 baculovirus could be seen on Fig. 3.3.B. After a series of infections starting as low as 0.02 µL and incubating for as long as 5 days, we pursued a different approach by incubating Sf9 cells with 2 µM UH15-38. Fortunately, introduction of the kinase inhibitor seemed to have acted as a chaperone, forcing RIPK3 in the conformation where no significant autophosphorylation occurred (Fig. 3.3. E).

3.3. Strategies to Improve Detection of Phosphorylated Sites of RIPK3

Autophosphorylated stock of RIPK3 was used on LCMS to elucidate the most optimal mode of analysis.

Table 3.2. LCMS Assessments with Phosphorylated RIPK3.

ATP	UH15-38	Coverage (%)	CID/ EAD	MVS	MVM	Inj. Vol (uL)	Guani.	Treatment
-	-	76.7	EAD	4140	51	40	+	Kit with Trypsin/ Lys-C
+	-	85.2	EAD	4042	65			
+	+	82.0	EAD	4068	52			
-	-	86.6	EAD	4474	141	35	-	Kit with Trypsin/ Lys-C
-	-	96.8	EAD	4214	170		+	
-	-	87.8	CID	6345	178		-	
-	-	99.1	CID	5823	221		+	
+	-	63.4	EAD	414	61	40	-	Kit with Trypsin/ Lys-C
+	-	76.5	EAD	2888	55		+	
+	-	84.6	CID	3020	35		-	
+	-	76.2	CID	2892	50		+	
-	-	89.5	EAD	6743	116		-	
-	-	96.8	EAD	6035	239		+	
-	-	85.8	CID	5426	118		-	
-	-	95.9	CID	5489	251		+	

While autophsopshorylated RIPK3 is not the best candidate to access the possible inhibition of RIPK3 p-sites by UH15-38, it could be used as positive control due to its abundance of phosphorylated residues. CID and EAD fragmentation modes were examined again, and CID in combination with guanidination seemed to provide both better coverage and higher MVS and MVM values. Results can be seen in Table 3.2 above.

Table 3.3. LCMS Assessments with RIPK3.

ATP	UH15-38	Coverage (%)	MVS	MVM	Guani.	Treatment	Phospho Modif. Detected	Rev. Volume of Phospho Modif. (%)
-	-	86.0	3868	126	-	Trypsin/ Lys-C FASP w/ C18 Column	T224, S227	N/A
+	-	88.7	3057	102	-		T224	
+	+	87.2	3851	115	-		T224, S227	
-	-	72.4	1211	27	+	Trypsin/ Lys-C FASP (n =1)	T224	12.81%
+	-	74.7	2233	59	+		T224, S227	58.08, 16.35%
+	+	72.7	1552	42	+		T224, S227	15.68, 3.69 %
-	-	58.7	2330	27	+	Trypsin/ Lys-C FASP (n=2)	T224	6.71%
+	-	49.4	1520	20	+		T224, S227	36.36, 8.38%
+	+	62.2	1623	25	+		T224	11.49%

Following the preparation of the new dephosphorylated RIPK3, another strategy was examined: filter aided sample preparation (FASP), a technique that is reported to assist with the cleanup and concentration of the protein sample. The rationale was that this will also assist with the detection of phosphopeptides in the absence of other easily available phospho-enrichment methods, such TiO2-based enrichment.[20] To implement the FASP method, the digestion protocol was altered such that reduction and alkylation steps were

performed on the filter, followed by overnight treatment with Trypsin/Lys-C, quenching with TFA and consequent elution of the sample off the FASP column. Two processing options were explored post elution: guanidination treatment or clean up with C18 spin column. All injection volumes were 50 µL at CID mode. The results are shown in Table 3.3 above.

Chapter 4: Discussion

4.1 Recombinant expression of human RIPK3 in Sf9 cells benefits from infection with UH15-38

In this thesis, we explored several approaches targeted at mitigating unwanted autophosphorylation of recombinant human RIPK3. Changing the amount of virus, used to infect Sf9 cells, or de-phosphorylating existing protein both prove to be either ineffective or unfeasible and resource heavy. It is unclear at this time why varying concentrations of imidazole that should competitively bind to Dynabeads instead of his-tagged protein, were uniformly inefficient at elution of RIPK3. On the other hand, utilizing an inhibitor, that is known to strongly associate with the protein of interest in vivo, as a chaperon of recombinant synthesis of said protein proved to be a reliable strategy, effectively solving the problem of autophosphorylation and possible misfolding of RIPK3.

4.2 Considerations for LCMS analysis of RIPK3 phosphorylation

FASP in tandem with C18 column did not provide substantial results for analysis, even though it had high coverage, MVS and MVMs. It could be likely because phoshphopeptides bind poorly to C18 resins, and thus might have been lost during wash steps. FASP with guanidination on the other hand seemed to produce highly abundant phosphopeptide fragments. The low coverage, MVS and MVMs could be due to sensitivity of the peptides to the abundance of salts as a small amount of precipitation was visible in most vials. With the warming, solids did go back into solution, however the LC-MS sampling rack is maintained at 15°C. As only the samples that were stored on the rack for prolonged time showed decreased amino acid coverage, warming to room temperature and gentle mixing of the sample right before the injection could be a possible solution to this

problem. Additionally, the analysis could benefit from utilizing fresh aliquots of a consistent stock of recombinant protein to avoid unaccounted premature degradation in analysis. Overall, here we show a method and parameters that could be used as a solid starting point for effective qToF LC-MS/MS phospho-peptide mapping of RIPK3.

4.3 Role of UH15-38 in inhibition of autophosphorylation of RIPK3

The final LCMS result is certainly interesting (Table 3.3), with observed quantifiable inhibition of pT224 and especially pS227. However, while it could explain the observed shift in bands on the Western blot that prompted this investigation, we cannot yet claim with certainty that UH15-38 acts specifically on these sites. Just like Gautam et al proposed, this could be a direct consequence of UH15-38 interacting with the back pocket of RIPK3, inhibiting the displacement of the αC helix, that in turn hinders association of RIPK3 with MLKL, as well as autophosphorylation events on RIPK3. While the phosphorylation signal was exceptionally good compared to previous runs, the relatively low percent coverage permits the possibility of missed phosphorylation sites. Further investigation is essential to either confirm or refute this hypothesis. The field presents an exciting area of research with significant potential for groundbreaking discoveries and new life-changing therapies.

Chapter 5. Appendix –LCMS CID Method

CID Sample Information

Data File Properties

Original data file name:	RIPK3 only_CID
Original data file path:	D:\SCIEX OS Data\Peptide mapping\Data\RIPK3 only_CID.wiff2
Original computer name:	DESKTOP-9DKMOAL
Software generated data file:	SCIEX OS 2.1.6.59781
Service version:	ClearCore2.Service 2.1.6

Device Properties

	Device Model	*Firmware Version*	*Serial Number*
MassSpectrometer	ZenoTOF™ 7600 System	AION_QTOF_ICX Version: 0 03 (0 04)	FB20372106
IntegratedSystem	ExionLC	3.71	ABCBM5974147
Valve	Valve Model	1.0.0.0	AB SCIEX 1

Batch File Properties

Batch file name: Untitled

Batch file path: N

MS Method File Properties

File name:	Peptide mapping 83min CID V2
File path:	D:\SCIEX OS Data\Peptide mapping
File locked:	False
File last modified date:	7/15/2023 11:41:10 PM

LC Method File Properties

File name:	Acquity CSH 100mm peptide mapping
File path:	D:\SCIEX OS Data\Peptide mapping

File locked:	False
File last modified date:	2/1/2023 2:44:10 PM

Sample Properties

Sample number in data file:	1
Type of acquisition:	Batch
Sample completion state:	Passed
Sample created at:	8/18/2023 7:07:22 AM
Sample last updated at:	8/18/2023 8:31:13 AM
Submitted by user:	DESKTOP-9DKMOAL\Tufts Medical
Actual Injection Volume (µl):	40
Rack code:	Control Rack
Rack position:	
Plate code:	1.5mL Control Rack (10 vial)
Plate position:	
Vial position:	7

Quantitation Properties

Sample Type:	Unknown
Dilution Factor:	1

Sample Info

External Device Properties

General

Contact Closure:	False
Calibrant Delivery System:	True

Method Parameters

General

Workflow:	Peptides (or other ≥2± analytes with MW < 5kDa)
Intact protein mode:	False
Method duration (minutes):	83
Total scan time (seconds):	2.503
Estimated cycles:	1990
Actual method duration (minutes):	83.49

Ion Source

Source name:	TurboIonSpray
Curtain gas:	35
CAD gas:	7
Ion source gas 1 (psi):	50
Ion source gas 2 (psi):	50
Temperature (°C):	450

Experiment

IDA Survey:

Scan type:	TOFMS
Polarity:	Positive
Ionspray voltage (V):	5500
TOF start mass (Da):	300

TOF stop mass (Da):	2500
Accumulation time (s):	0.2
Declustering potential (V):	80
Declustering potential spread (V):	0
Collision energy (V):	10
Collision energy spread (V):	0
Time bins to sum:	8
Channel 1:	True
Channel 2:	True
Channel 3:	True
Channel 4:	True
Override QJet RF value:	False
QJet RF amplitude (V):	227.243869443398

IDA Criteria:

Workflow:	Peptide
Maximum candidates ion:	30
Intensity threshold exceeds (counts/s):	125
Dynamic Background Subtract:	False
Exclude former candidate ions:	True
For (sec):	6
After (occurrences):	2

Dynamic CE for MS/MS: True

CE Equation: CE = (slope) * (m/z) + (intercept)

Charge state of zero: Applied when charge state is unknown

Charge	*Slope*	*Intercept*
0	0.049	-1
1	0.05	5
2	0.049	-1
3	0.048	-2
4	0.05	-2
5	0.05	-2
6	0.05	-2
7	0.05	-2
8	0.05	-2
9	0.05	-2
10	0.05	-2
11	0.05	-2
12	0.05	-2

Maximum CE (V): 80

Minimum CE (V): 5

Dynamic ETC for MS/MS: False

Charge state:	True
From:	2
To:	4
Isotope to select:	Most intense

Advanced IDA criteria:

ExcludeIsotope:	False
Mass tolerance +/- (ppm):	100
Candidate mass range:	False
Adjust CE when using iTRAQ reagent:	False

Inclusion list:	False
Exclusion list:	False
Mass Defect Filter:	False
Isotope Matching:	False
Neutral Loss:	False

IDA Dependent:

Scan type:	TOFMSMS
Polarity:	Positive

Ionspray voltage (V):	5500
Fragmentation mode:	CID
TOF start mass (Da):	100
TOF stop mass (Da):	3000
Accumulation time (s):	0.07
Declustering potential (V):	80
Declustering potential spread (V):	0
Collision energy spread (V):	0
Q1 resolution:	Unit
Zeno pulsing:	True
Zeno threshold (cps):	100000
Time bins to sum:	8
Channel 1:	True
Channel 2:	True
Channel 3:	True
Channel 4:	True
Override QJet RF value:	False
QJet RF amplitude (V):	202.72

Chapter 6. Bibliography

1. Galluzzi L, Vitale I, Aaronson SA, et al. Molecular mechanisms of cell death: recommendations of the Nomenclature Committee on Cell Death 2018. Cell Death Differ 2018;25:486-541.
2. Yuan J, Ofengeim D. A guide to cell death pathways. Nat Rev Mol Cell Biol 2024;25:379-395.
3. Wu XN, Yang ZH, Wang XK, et al. Distinct roles of RIP1-RIP3 hetero- and RIP3-RIP3 homo-interaction in mediating necroptosis. Cell Death Differ 2014;21:1709-1720.
4. Ye K, Chen Z, Xu Y. The double-edged functions of necroptosis. Cell Death Dis 2023;14(2):163.
5. Puylaert P, Coornaert I, Neutel CHG, et al. The Impact of RIPK1 Kinase Inhibition on Atherogenesis: A Genetic and a Pharmacological Approach. Biomedicines 2022;10(5):1016.
6. Cuny GD, Degterev A. RIPK protein kinase family: Atypical lives of typical kinases. Semin Cell Dev Biol 2021;109:96-105.
7. Gautam A, Boyd DF, Nikhar S, et al. Necroptosis blockade prevents lung injury in severe influenza. Nature 2024;628:835-843.
8. Gardner CR, Davies KA, Zhang Y, et al. From (Tool)Bench to Bedside: The Potential of Necroptosis Inhibitors. J Med Chem 2023;66(4):2361-2385.
9. Günther C, Martini E, Wittkopf N, et al. Caspase-8 regulates TNF-α-induced epithelial necroptosis and terminal ileitis. Nature 2011;477:335-339.

10. Nogusa S, Thapa RJ, Dillon CP, et al. RIPK3 Activates Parallel Pathways of MLKL-Driven Necroptosis and FADD-Mediated Apoptosis to Protect against Influenza A Virus. Cell Host Microbe 2016;20(1):13-24.

11. Loughrey Chen S, Huddleston MJ, Shou W, Deshaies RJ, Annan RS, Carr SA. Mass spectrometry-based methods for phosphorylation site mapping of hyperphosphorylated proteins applied to Net1, a regulator of exit from mitosis in yeast. Mol Cell Proteomics 2002;1(3):186-196.

12. Sui S, Wang J, Yang B, et al. Phosphoproteome analysis of the human Chang liver cells using SCX and a complementary mass spectrometric strategy. Proteomics 2008;8(10):2024-2034.

13. Iliuk AB, Arrington JV, Tao WA. Analytical challenges translating mass spectrometry-based phosphoproteomics from discovery to clinical applications. Electrophoresis 2014;35(24):3430-3440.

14. Blackburn K, Goshe MB. Challenges and strategies for targeted phosphorylation site identification and quantification using mass spectrometry analysis. Brief Funct Genomic Proteomic 2009;8(2):90-103.

15. Garnish SE, Meng Y, Koide A, et al. Conformational interconversion of MLKL and disengagement from RIPK3 precede cell death by necroptosis. Nat Commun 2021;12:2211.

16. Meng Y, Horne CR, Samson AL, et al. Human RIPK3 C-lobe phosphorylation is essential for necroptotic signaling. Cell Death Dis 2022;13:565.

17. Luo Y, Matejic T, Ng C-K, et al. 8 - Characterization and Analysis of Biopharmaceutical Proteins. Separation Science and Technology 2011;10:283-359.

18. Sun M, Liang Y, Li Y, et al. Comprehensive Analysis of Protein N-Terminome by Guanidination of Terminal Amines. Anal Chem 2020;92:567-572.

19. Parker CE, Mocanu V, Mocanu M, et al. Mass Spectrometry for Post-Translational Modifications. Neuroproteomics. Boca Raton (FL): CRC Press/Taylor & Francis 2010; Chapter 6. Available from: https://www.ncbi.nlm.nih.gov/books/NBK56012/

20. Wiśniewski JR, Nagaraj N, Zougman A, Gnad F, Mann M. Brain phosphoproteome obtained by a FASP-based method reveals plasma membrane protein topology. J Proteome Res 2010;9(6):3280-3289.